Experimental Neurology 316 (2019) 12–19

Contents lists available at ScienceDirect

Experimental Neurology

journal homepage: www.elsevier.com/locate/yexnr

Research Paper

MicroRNA-132 attenuates cerebral injury by protecting blood-brain-barrier in MCAO mice

Xiaokun Zuo[a,b], Jianfei Lu[b], Anatol Manaenko[c], Xin Qi[b], Jiping Tang[d], Qiyong Mei[e,*], Ying Xia[a,*], Qin Hu[b,*]

[a] Department of Neurosurgery, Affiliated Haikou Hospital, Xiangya Medical College of Central South University, Haikou, China
[b] Discipline of Neuroscience, Department of Anatomy, Histology and Embryology, Shanghai Jiao Tong University School of Medicine, Shanghai, China
[c] Departments of Neurology, University of Erlangen-Nuremberg, Erlangen, Germany
[d] Department of Physiology, Loma Linda University School of Medicine, Loma Linda, CA, USA
[e] Department of Neurosurgery, Changzheng Hospital, the Second Military Medical University, Shanghai, China

ARTICLE INFO

Keywords:
MicroRNA-132
MMP-9
BBB integrity
Ischemic stroke

ABSTRACT

MicroRNAs (miRNAs) have been widely reported to induce posttranscriptional gene silencing and led to an explosion of new strategies for the treatment of human disease. It has been reported that the expression of MicroRNA-132 (miR-132) are altered both in the blood and brain after stroke. However, the effect of miR-132 on blood-brain barrier (BBB) disruption in ischemia stroke has not been studied. Here we will investigate the effects of miR-132 on the permeability of BBB after ischemic stroke and explore the potential mechanism underlying observed protection. Eight week-old mice were injected intracerebroventricularly with miR-132, antagomir-132 or agomir negative control (agomir-NC) 2 h before middle cerebral artery occlusion (MCAO), followed by animal behavior tests and infraction volume measurement at 24 h after MCAO. BBB permeability and integrity were measured by Evan's blue extravasation and brain water content. The expression of tight junction proteins was detected by immnostaining and Western blots. The level of MiR-132 and its targeted gene Mmp9 were assayed. Treatment with exogenous MiR-132 (agomir-132) decreased the infraction volume, reduced brain edema, and improved neurological functions compared to control mice. Agomir-132 increased the level of MiR-132 in brain tissue, suppressed the expression of MMP-9 mRNA and decreased the degradation of tight junction proteins VE-cadherin and β-Catenin in ischemic stroke mice. Inhibition of MMP-9 has a similar protective effect to agomir-132 on infraction volume, brain edema, and tight-junction protein expression after MCAO. Our results indicated that miR-132/MMP-9 axis might be a novel therapeutic target for BBB protection in ischemic stroke.

1. Introduction

Stroke is a devastating cerebrovascular disease with high rates of permanent disability and mortality. About 80% of strokes are ischemic strokes, caused by blockage of the artery supplying the brain (Koh and Park, 2017). Currently thrombolysis with tPA and mechanical thrombectomy are the only effective therapeutic approaches for treatment of acute ischemic stroke patients, however, both are limited by the narrow therapeutic window (Lapchak et al., 2017; Lapchak and Zhang, 2017). Giving the fact, that vast majority of neuroprotective agents, positively tested in pre-clinic studies have failed in clinical trials, it is urgently needed to identify novel therapeutic targets and find the alternative therapy for ischemic stroke (Cassidy and Cramer, 2017; Lim and Spector, 2017).

MicroRNAs (miRNAs) have been widely reported to induce post-transcriptional gene silencing thus led to an explosion of new strategies for the treatment of human disease (Li et al., 2018). In central nervous system, various pathological conditions such as neurodegernerative diseases, stroke, and schizophrenia significantly altered cerebral miRNA profiles and affect the disease outcome (El Fatimy et al., 2018; Huang et al., 2016; Miller et al., 2012). It is well established that the expression of miR-132 are altered both in the blood and brain after stroke (Bell et al., 2017; Huang et al., 2016; Rink and Khanna, 2011). Previous study had identified MicroRNA-132 (miR-132) as a key regulator of angiogenesis in larval zebrafish, regulating the expression of the vascular junction protein Cdh5 (also known as VE-cadherin) by targeting *eef2k* (Xu et al., 2017). In another experiment, miR-132 severed as an inhibitor of Acetyl cholinesterase and restrained

* Corresponding authors.
E-mail addresses: meiqiyong@smmu.edu.cn (Q. Mei), huqin@shsmu.edu.cn (Y. Xia), xiaying008@163.com (Q. Hu).

https://doi.org/10.1016/j.expneurol.2019.03.017
Received 9 December 2018; Received in revised form 24 March 2019; Accepted 27 March 2019
Available online 28 March 2019
0014-4886/

inflammation after intracerebral hemorrhage (Zhang et al., 2017). However, to date the effect of miR-132 on blood-brain barrier (BBB) disruption in ischemic stroke has not been reported. Here we will investigate the effects of miR-132 on the permeability of BBB after ischemic stroke and explore the potential mechanisms.

2. Materials and methods

2.1. Animals and experimental design

The study was approved by Animal Care and Use, Committee of Shanghai Jiao Tong University School of Medicine, Shanghai, China (No. A2015-011). Male C57BL/6 mice weighing 20–25 g were purchased from Shanghai Slac Laboratory Animal Company, China. Mice were randomly divided into five groups: sham operation, middle cerebral artery occlusion (MCAO), MCAO + miR-132 group (MCAO + agomir-132), MCAO + miR-132 antagonist group (MCAO + antagomiR-132) and MCAO + miR-132 negative control group (MCAO + agomir-NC) and an additional MCAO + MMP-9 inhibitor group. Agomir-132, antagomiR-132 and agomir-NC were synthesized by Sangon Biotech, Shanghai, China. MMP-9 inhibitor (ab142180) was purchased from abcam.

2.2. MCAO model

Transient MCAO was induced as previously described (Hu et al., 2017). The mice were deeply anesthetized with 2% chloralhydrate (1 ml/100 g, intraperitoneal injection). A middle line incision was made at the neck, and the left carotid artery was separated carefully. Then a monofilament suture (702234PK5Re, Doccol, Sharon, MA, USA) was inserted into the left internal carotid artery. Rectal temperature was maintained at 37.0 °C during and after surgery with a temperature-control heating pad. Animal regional cerebral blood flow (rCBF) was monitored by transcranial laser Doppler (moor VMS-LDF2, Moor Instruments, UK), and animals with rCBF higher than 20% of original baseline value was excluded from the study. The monofilament suture was removed slowly 1 h after occlusion. Mice were housed under controlled temperature and photoperiod conditions (12 h light/dark), with food and water freely available.

2.3. Intracerebroventricular injection

Agomir-132, antagomir-132, agomir-NC (0.8 nmol dissolved in 4 μl PBS) and MMP-9 inhibitor (0.002 nmol dissolved in 4 μl PBS) were applied 2 h before MCAO via intraventricular injection (ICV). The injections were performed as previously described (Hu et al., 2017). Mice were anesthetized and positioned lying prone in a stereotactic head frame (RWD Life Science, China). A scalp incision was made along the midline and a burr hole was drilled into the right side of the skull (0.5 mm posterior and 1.0 mm lateral to the bregma). miR-132, antagomiR-132, miR-NC or MMP-9 inhibitor (4 μl) were microinfused into right lateral ventricles through a Hamilton syringe (2.5 mm vertically), which was driven by a microinfusion pump (KDS 310, KD Scientific) with 0.2 μl/min. The needle was left in place for an additional 5 min after injection to prevent possible leakage and was slowly withdrawn within 4 min. After the needle was removed, the burr hole was sealed with bone wax; the incision was closed with sutures and the mice were allowed to recover.

2.4. 2,3,5-triphenyltetrazolium hydrochloride (TTC) staining

After 24-h reperfusion, the brain was collected, sectioned coronally at 1 mm interval, stained with TTC at 37 °C for 20 min. Then, brain sections were fixed in 2% paraformaldehyde and photographed with a digital camera (Canon IXUS175, Tokyo, Japan). The possible interference of brain edema on infarct volume was corrected (whole contralateral hemisphere volume − nonischemic ipsilateral hemisphere volume) and the infracted volume was expressed as a ratio of the whole contralateral hemisphere.

2.5. Neurological scores

After 24-hour reperfusion, neurological function was scored in a blind manner as previous described (Hu et al., 2017). Six grades were involved in Garcia score containing spontaneous activity, spontaneous movements of all limbs, movements of forelimbs, climbing wall of wire cage, touch of trunk and Vibrissae touch, with the minimum score 0 (severest deficit), and the maximum score 3 (normal).

2.6. Foot-fault test

For testing of motor coordination, foot-fault test was performed by a blinded investigator 24 h after MCAO as previously described (Hu et al., 2017). Mice were placed on a horizontal grid floor elevated above the surface and allowed to walk for 2 min. A foot fault was noted when the mouse's foot miss–stepped on the grid and the foot fell downwards through the opening between the grids. All four limbs were observed for misses. The percentage of total foot faults was recorded for statistical analyses.

2.7. Measurement of Evans Blue leakage extravasation

2% Evans Blue dye (EB, Sigma, Shanghai, China) (2 ml/kg) was used as a tracer after MCAO operation by intraperitoneal injection. After 24-hour reperfusion, the brain was collected, sectioned coronally at 1 mm interval and photographed. After intracardial perfusion with PBS, brains were removed and weighed on an electronic balance; the ipsilateral hemisphere was homogenized into a test tube with 1 ml PBS. Supernatants were collected after centrifugation. 0.5 ml trichloroacetic acid (TCA) (500 g in 227 ml ddH_2O) was added to same volume of the supernatant, followed by overnight incubation in 4 °C. After centrifugation, supernatants were collected. Nine groups of EB concentration by gradient dilution and its Optical Density (OD) at 620 nm were plotted by a multi-mode reader (BioTek, SYNERGY, USA) and the standard curve of EB concentration and OD was calculated by Excel 2010 (Microsoft) (Supplementary Fig. 3). OD of the supernatants was measured at 620 nm by using the multi-mode reader (BioTek, SYNERGY, USA). The concentration of EB was calculated. OD was transited to EB concentration by the curve and then revised by brain weight.

2.8. Brain water content

Mice were intraperitoneally anesthetized and the brain was quickly divided into right hemisphere, left hemisphere and cerebellum. The tissues were weighed immediately before placing in an oven (WS70-1) at 105 °C for 48 h to attain dry weight. Brain water content of each part was calculated as follow: wet to dry (W/D) ratio = [(wet weight − dry weight)/wet weight] × 100%.

2.9. Real-time PCR

After 24-hour reperfusion, the total RNA was extracted from the brain using TRIzol reagent (Invitrogen, Carlsbad, CA, USA) according to manufacturer's instructions and then processed for reverse-transcription into cDNA in a 20-μL mixture containing 1 μg of total RNA using miRcute miRNA First-Strand cDNA (Tiangen, Beijing, China). The following primers were used (Tiangen, Beijing, China): U6, CTC GCT TCG GCA GCA CA (forward) and AAC GCT TCA CGA ATT TGC GT (reverse); miR-132, GCC CGT AAC AGT CTA CAG CCA T (forward) and GCA GGG TCC GAG GTA TTC (reverse). The microRNA was detected using miRcute miRNA qPCR Detection Kit (Tiangen, Beijing, China) by Power

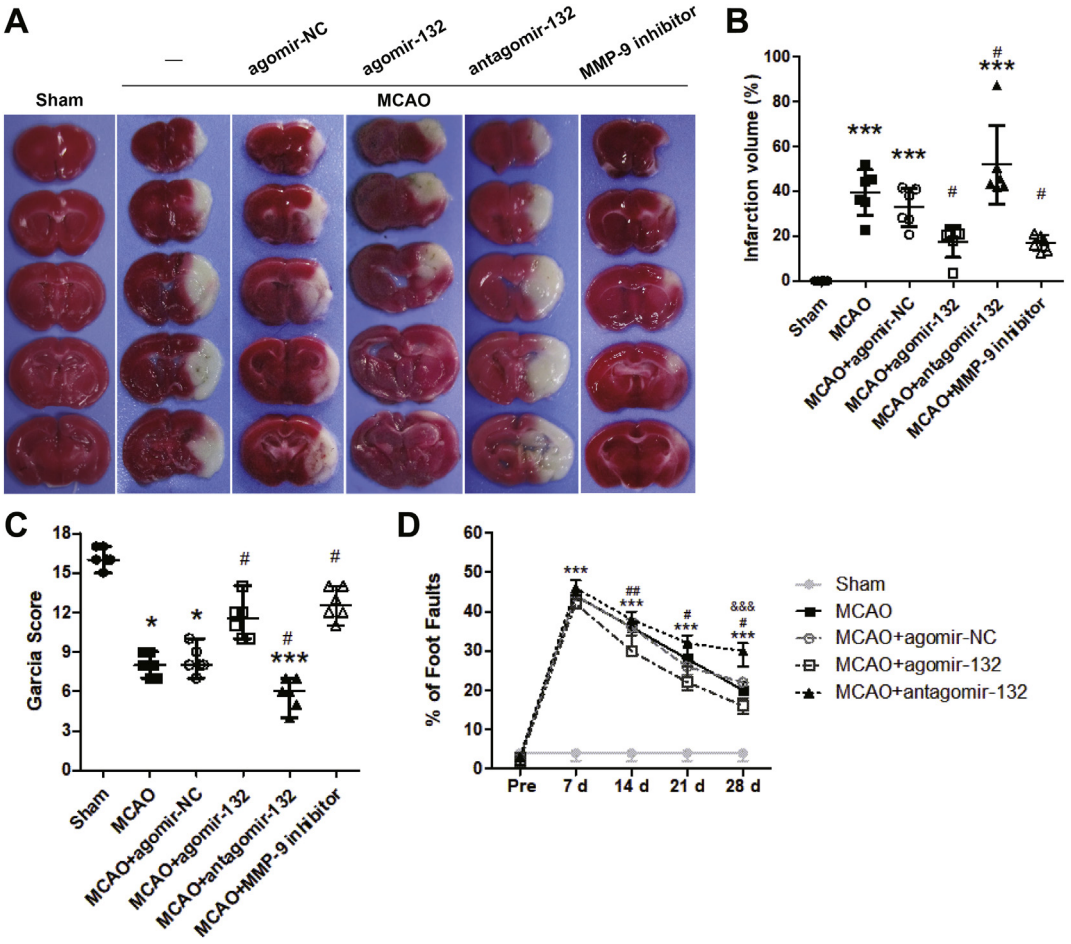

Fig. 1. Administration of agomir-132 reduced the infarction and improved neurological deficits in MCAO mice. (A) Representative images of brain slices stained by TTC in different groups at 24 h after MCAO. (B) Quantitative analysis of infarction volume in different groups. (C) Neurological scores in different groups evaluated at 24 h after MCAO. (D) Foot fault test at pre-MCAO and day 7, 14, 21, 28 post-MCAO for different treated groups. $^{*}p < .05$ vs. Sham, $^{***}p < .001$ vs. Sham, $^{\#}p < .05$ vs. MCAO + agomir-NC, $^{\#\#}p < .05$ vs. MCAO + agomir-NC $^{\&\&\&}p < .001$ in MCAO + antagomir-132 vs MCAO + agomir-NC. Values are presented as Mean ± SD or Median with range for enumeration data, $n = 6$ per group.

SYBR Green PCR Master Mix (Thermo Fisher Scientific, Hemel Hempstead, UK), and U6 served as an internal reference.

2.10. Western blot assay

Mice were sacrificed, and the brain was collected. Whole-cell protein was prepared from the ischemic cortices divided from left cerebral hemisphere. In brief, brain tissues were homogenized in RIPA buffer (P1003B, Beyotime, wuhan, China) containing protease inhibitor cocktail (P8340, Sigma, St. Louis, MO, USA), and then sonicated on ice. After centrifugation, the supernatant was collected for western blot assay. An aliquot of 20 μg mg protein from each sample was separated by SDSPAGE and then transferred onto a nitrocellulose membrane. The membrane was blocked with 5% nonfat milk in TBST for 2 h (pH 7.4) and then incubated with primary antibodies against Occludin (1:1000; ab216327, abcam), β-catenin (1:1000; ab32572, abcam), VE-cadherin (1:1000; ab205336, abcam) or β-actin (1:1000; 4967S, Cell Signaling Technology) at 4 °C overnight. After incubation with secondary antibody for 2 h at room temperature, visualization was done with a chemiluminescence apparatus (ImageQuant LAS 4000mini, GE Healthcare, USA). The gray value of Occludin, β-catenin and VE-cadherin was measured with Image-J software, and normalized to that of β-actin as the relative protein expression.

2.11. Luciferase reporter assay

Fragment of Mmp9 gene 3′-UTR (wild-3′-UTR) containing a miR-132 targeting site and its respective mutant were amplified by PCR and cloned into the psiCHECK-2 vector (C8021, Promega, USA). CHO cells were co-transfected in 24-well plates with 0.5 μg of the dual-luciferase reporter vector and 100 nM agomir-132, agomir-NC or antagomir-132 using 2.5 μl HilyMax transfection reagent (H357, Dojindo, Japan). Luciferase assays were performed with a Dual-Luciferase Reporter Assay System (E1910, Promega, USA) 48 h after transfection according to the manufacturer's protocol. Renilla luciferase activity was normalized to that of firefly luciferase.

2.12. Gelatin zymography

Gelatinase activities were measured using a Novex™ Zymogram Plus Gels (MAN0016629, Thermo Fisher, USA) following the manufacturer's instructions. Cerebral cortices in the ipsilateral side 24 h after MCAO were solubilized in lysis buffer, containing 25 mM Tris (pH 7.6), 150 mM NaCl, and 1% NP-40, and kept at −80 °C until immediately before use. PAGE was performed using a gelatin-containing gel. Gels were incubated in reacting buffer for 48 h at 37 °C after incubation, and in renaturing buffer for 1 h at room temperature. Matrix metalloproteinase (MMP) activity was visualized as clear bands against the Coomassie brilliant blue stained gelatin background. The intensity of each band was quantified using Image J.

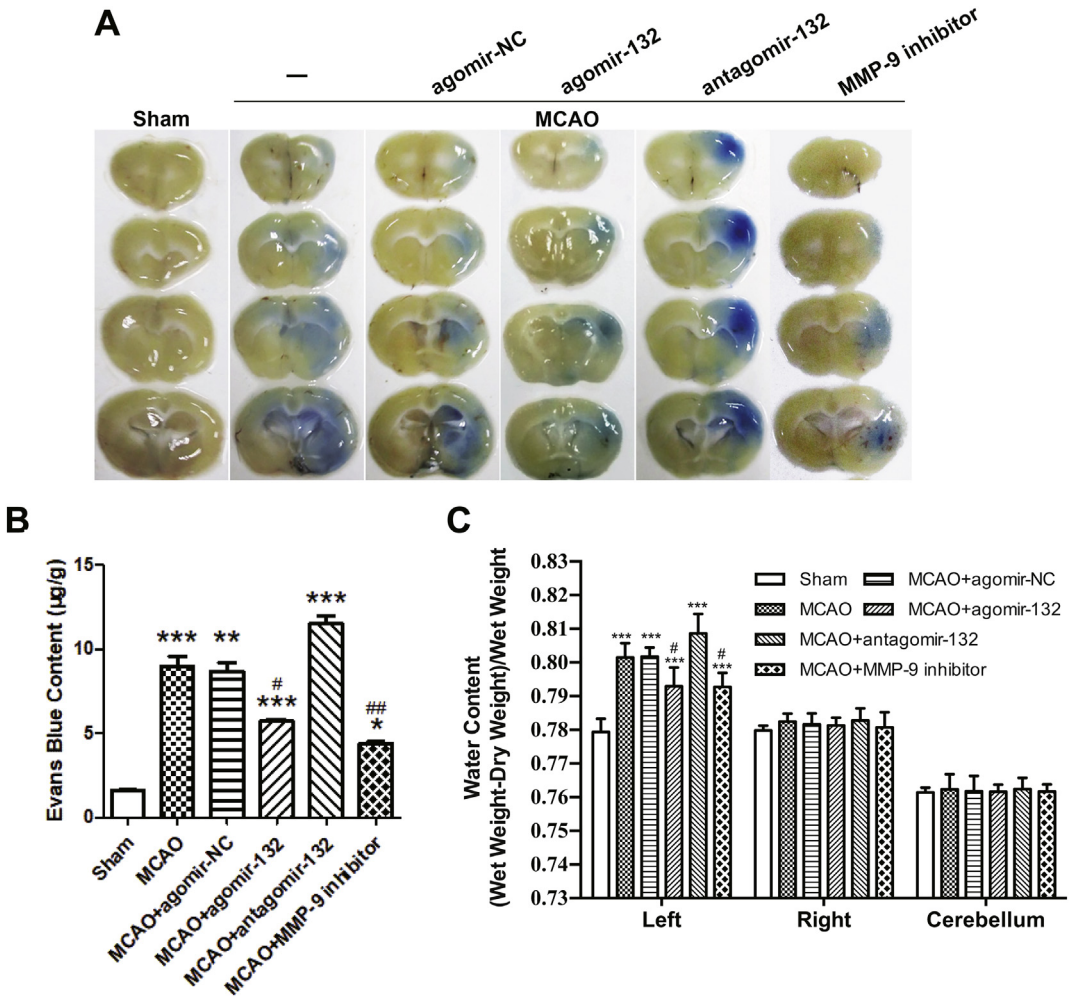

Fig. 2. Treatment of agomir-132 attenuated blood-brain barrier leakage after MCAO. (A) Representative images of Evans blue staining in different groups at 24 h after MCAO. (B) Quantitative analysis of Evans blue leakage in different groups. (C) Brain water content in different groups at 24 h after MCAO. $^{*}p < .05$ vs. Sham, $^{***}p < .001$ vs. Sham, $^{\#}p < .05$ vs. MCAO + agomir-NC, $^{\#\#}p < .01$ vs. MCAO + agomir-NC. Values are presented as Mean ± SD, n = 6 per group. (For interpretation of the references to color in this figure legend, the reader is referred to the web version of this article.)

2.13. Immunofluorescence

One day after MCAO, the mice were anesthetized and perfused intracardially with PBS followed by 4% paraformaldehyde as previously described (Hu et al., 2017). Brains were removed, post-fixed in 4% paraformaldehyde for 24 h, and dehydrated in a 30% sucrose solution for 3–5 days at 4 °C. Free-floating coronal brain slices (20 μm thick) were cut using a cryostat and stored at −20 °C until used. Sections were rinsed with PBS and permeabilized with 0.3% Triton X-100 in PBS for 30 min. Specimens were blocked with 10% goat serum for 1 h and incubated at 4 °C overnight with a primary rabbit polyclonal anti-VE-cadherin antibody (1:200; ab205336, abcam) and a primary mouse monoclonal anti-CD-31 antibody (1:50; ab9498, abcam) followed by an Alexa 488-labeled goat anti-rabbit IgG (1:500, Beyotime, Wuhan, China) and an Alexa 568-labeled goat anti-mouse IgG respectively for 2 h at 37 °C. DAPI was applied to stain all the nuclei as a background staining. Imaging was performed on a laser scanning confocal microscope (Eclipse TE2000U; Nikon) with the Nikon EZ-C1 software.

2.14. Nissl staining

Mice were anesthetized at 28 days after MCAO and then transcardially perfused with PBS followed by 2% paraformaldehyde solution. Brains were harvested and postfixed in paraformaldehyde overnight. Whole brains were photographed with a digital camera (Canon IXUS175, Tokyo, Japan), and 40-μm thick coronal sections were collected by VIBRATOME LINE (LEICA VT 1000 S) for Nissl staining. Brain sections were dehydrated in serial alcohol and a quick rinse in distilled water, and then immersed in 0.1% cresyl violet for 20 min at room-temperature. Sections were dehydrated in serial alcohol again and xylene before cover slipping with mounted medium. Sections were then photographed by a microscope (OLYMPUS IX71), and whole brain image were synthesized by several images of partial visual field on cellSens Dimension.

2.15. Statistical analyses

The analysis of the data was performed using GraphPad Prism software. Multiple comparisons were statistically analyzed with one-way analysis of variance (ANOVA) followed by the Tukey method or non-parametric test. The data are presented as means ± SEM or median ± range, and a value of $p < .05$ represents statistical significance.

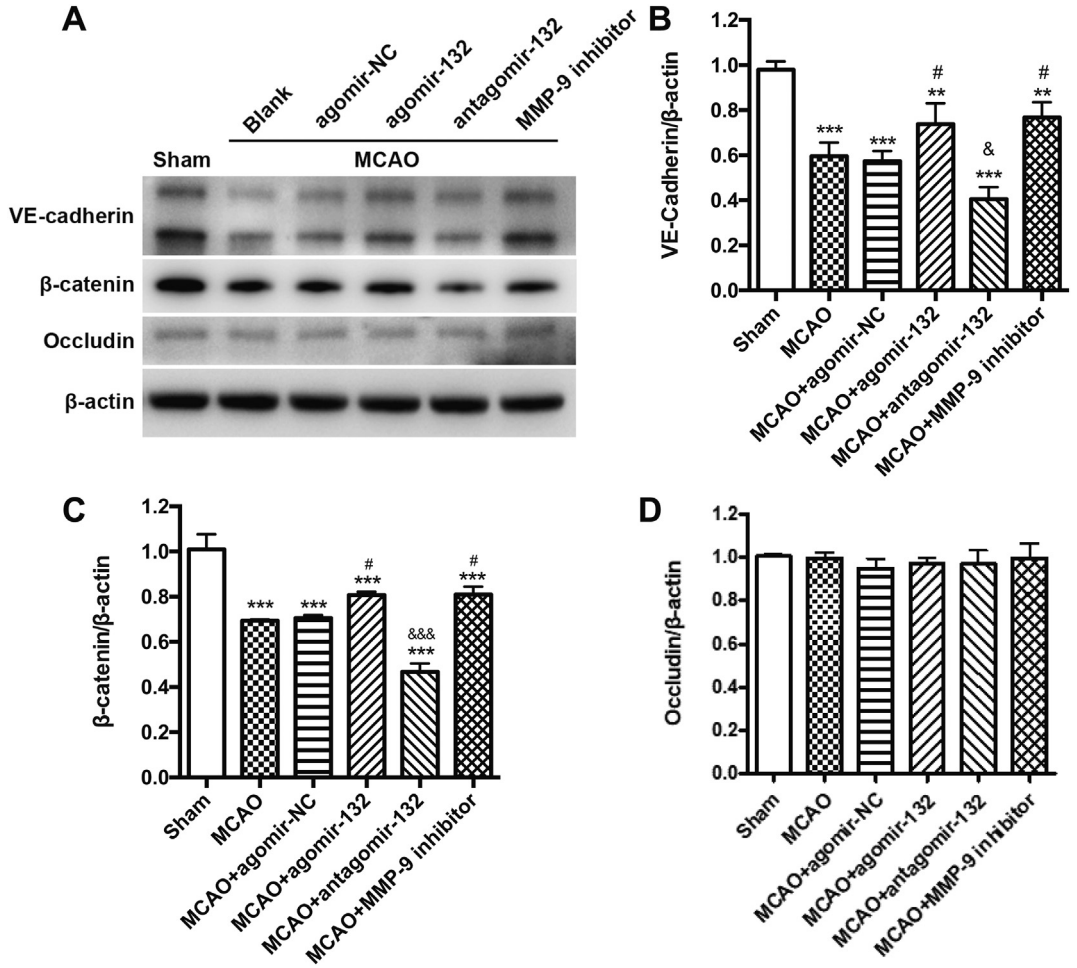

Fig. 3. Effects of agomir-132 on the expression of junction proteins after MCAO. (A) Western blot indicated agomir-132 attenuate the decrease of VE-cadherin and β-catenin after MCAO but have no effects on Occludin. (B)&(C)&(D) Quantitative analysis of VE-cadherin, β-catenin and Occludin in different groups. $^{**}p < .01$ vs. Sham, $^{***}p < .001$ vs. Sham, $^{\#}p < .05$ vs. MCAO + agomir-NC, $^{\&}p < .05$ in MCAO + antagomir-132 vs MCAO + agomir-NC, $^{\&\&\&}p < .001$ in MCAO + antagomir-132 vs MCAO + agomir-NC. Values are presented as Mean ± SD, n = 6 per group.

3. Results

3.1. Administration of exogenous agomir-132 reduced infarction volume and improved neurological deficits

TTC staining was used to reveal cerebral infarct, whereas normal brain tissue is stained red and the infarct lesion remains unstained (white color) (Fig. 1A). MCAO for 1 h caused a significant brain infarction and deteriorated neurobehavior at 24 h after surgery (Fig. 1A, B & 1C, $p < .001$ vs. Sham group), and administration of agomir-132 effectively reduced the infarct volume and improved the neurological scores (Fig. 1A, B & 1C $p < .05$ vs. MCAO + agomir-NC group). To further confirm the role of miR-132 in ischemic stroke, we synthesized anti-miR-132 (antagomir-132) that specific to silence endogenous miR-132, and found that antagomir-132 abolished the protective effect of agomir-132 (Fig. 1A, B & 1C, $p < .05$ vs. MCAO + agomir-NC group). There were no significant difference of infract volume between MCAO group and MCAO + agomir-NC group. No infarction was found on agomir-132 or antagomir-132 2 h pre-treated sham group mice (Supplementary Fig. 1). In addition, inhibition of MMP-9 in MCAO also reduced the infarct volume and improved the neurological scores (Fig. 1A, B & 1C, $p < .05$ vs. MCAO group). In the long-term, administration of agomir-132 greatly ameliorated the performance of foot-fault test at 28 days after MCAO (Fig. 1D $p < .05$ vs. MCAO + agomir-NC group), which was reversed by antagomir-132 (Fig. 1D, $p < .01$ vs. MCAO + agomir-NC group). Brain injury/recovery condition at day 28 was presented in Supplementary Fig. 3.

3.2. Administration of agomir-132 preserved the integrity of BBB

The amount of Evan's blue dye extravasation in the left cerebral hemisphere was markedly increased after 24 h of MCAO (Fig. 2A & 2B, $p < .01$ vs. Sham group). Pre-treatment with agomir-132 significantly attenuated the extravasation of Evan's blue in the ischemia hemisphere (Fig. 2A & 2B, $p < .01$ vs. MCAO + agomir-NC group), and pre-treatment with antagomir-132 exacerbated the extravasation of Evan's blue at 24 h after MCAO (Fig. 2A & 2B $p < .01$ vs. MCAO + agomir-NC group). Meanwhile, agomir-132 largely reduced the brain water content in the ischemic hemisphere (Fig. 2C $p < .05$ vs. MCAO + agomir-NC group), and antagomir-132 increased the brain water content at 24 h after MCAO (Fig. 2C, $p < .01$ vs. MCAO group). These findings demonstrated that pre-treatment with agomir-132 attenuated the BBB broken in ischemic stroke. MMP-9 inhibition group showed a similar function to agomir-132, attenuating the extravasation of Evan's blue (Fig. 2A & 2B, $p < .01$ vs. MCAO + agomir-NC group) and reducing the brain water content in the ischemia hemisphere (Fig. 2C, $p < .05$ vs. MCAO + agomir-NC group).

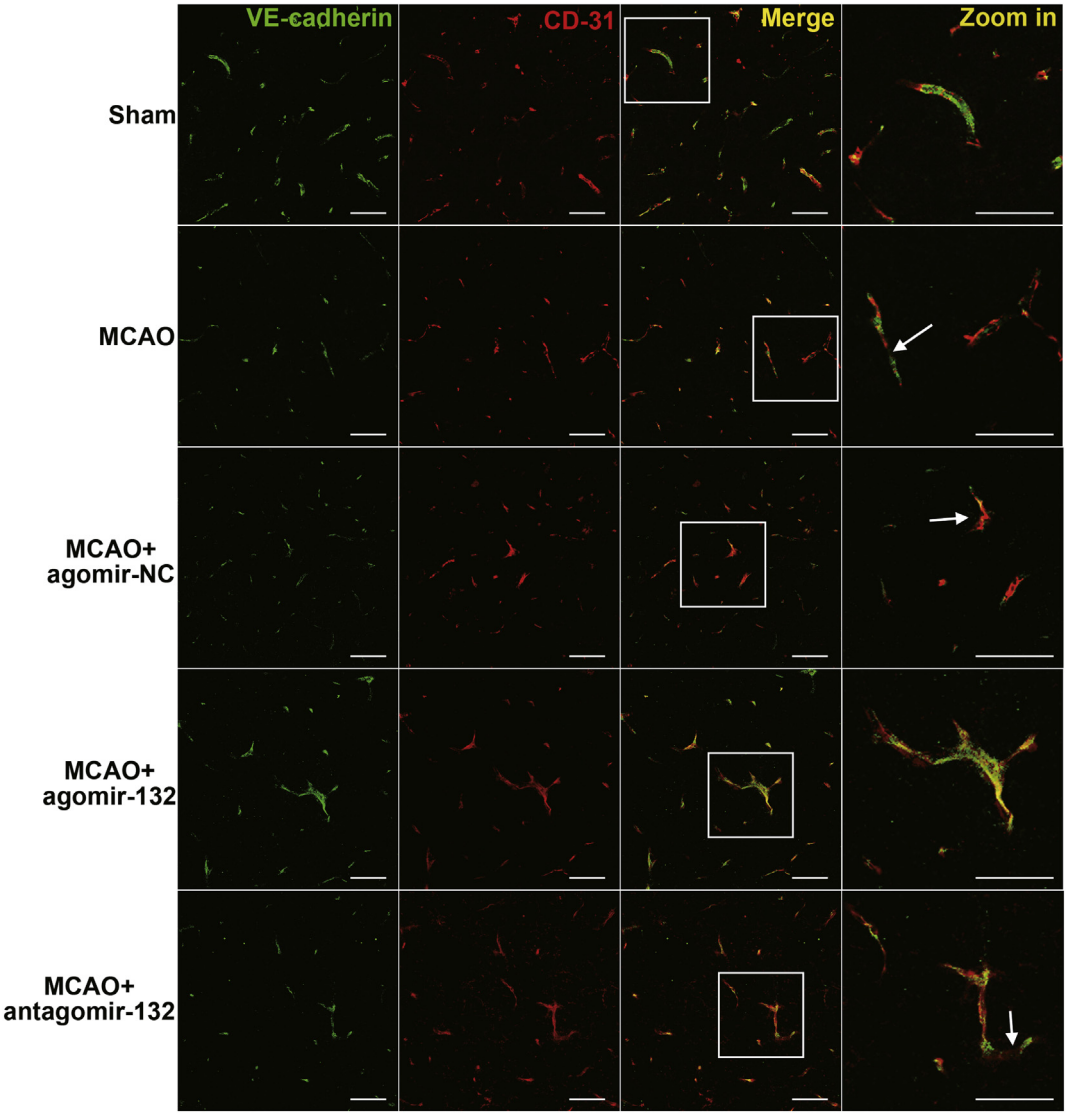

Fig. 4. Representative immunofluorescence images of VE-cadherin in endothelial cells at 24 h after MCAO. CD31 is the marker of endothelial cells. Arrows indicated the uncontinuous cell junction. Bar = 50 μm, $n = 5$ per group.

3.3. Treatment with agomir-132 attenuated the degradation of tight junction proteins

To gain insight into the rationale behind the role of miR-132 in maintaining BBB integrity, vascular endothelial tight junction associated proteins were examined by Western blots and immunofluorescence staining. The expression of VE-cadherin and β-catenin were greatly decreased in the ischemic hemisphere at 24 h after MCAO (Fig. 3A, B & 3C $p < .01$ vs. MCAO + Sham group); administration of agomir-132 preserved the expression of VE-cadherin and β-catenin (Fig. 3A, B & 3C, $p < .05$ vs. MCAO + agomir-NC group), and the effects was abolished by antagomir-132 (Fig. 3A, B & 3C, $p < .05$ vs. MCAO + agomir-NC group). There was no significant difference in the expression of Occludin in the ischemic hemisphere after MCAO and neither agomir-132 nor antagomir-132 affected its expression (Fig. 3A &3D). Administration of MMP-9 inhibitor also preserved the expression of VE-cadherin and β-catenin (Fig. 3A, B & 3C, $p < .01$ vs. MCAO group). Double immunofluorescence staining of VE-cadherin and CD-31 (marker of endothelial cells) showed that the expression of VE-cadherin in microvessels decreased at 24 h after MCAO, pretreatment with agomir-132 prevented the degradation of VE-cadherin and maintained the integrity of BBB (Fig. 4).

3.4. MMP-9 severed as a direct down-stream target of miR-132

Bioinformatics analysis including TargetScan database were used to predict putative target of miR-132 and MMP-9 was predicted as its target (Fig. 5A). Co-transfection of the dual-luciferase reporter plasmid containing Mmp9 3′UTR with agomir-132 decreased the reporter activity in CHO (Fig. 5B). Moreover, Gelatinase assay revealed the gelatinase activity around 90 kDa, which represents MMP-9, remarkably increased in MCAO, agomir-NC and antagomir-132 groups compared with Sham group (Fig. 5D & E). While in agomir-132 group the gelatinase activity just had a significant decrease slight increase. (Fig. 5D & E). These data indicated that MMP-9 is a direct target of miR-132. Brain tissue Brain parenchyma miR-132 was detected by real-time PCR and was significantly increased in agomir-132 group (Fig. 5C, $p < 0.001$ vs. MCAO + agomir-NC). On the contrary, intracerebroventricular injection of antagomir-132 reduced miR-132 level (Fig. 5C, $p < 0.01$ vs. MCAO + agomir-NC).

4. Discussion

In the present study we demonstrated that miR-132 is protective after MCAO on mice and explored the molecular pathway underlying

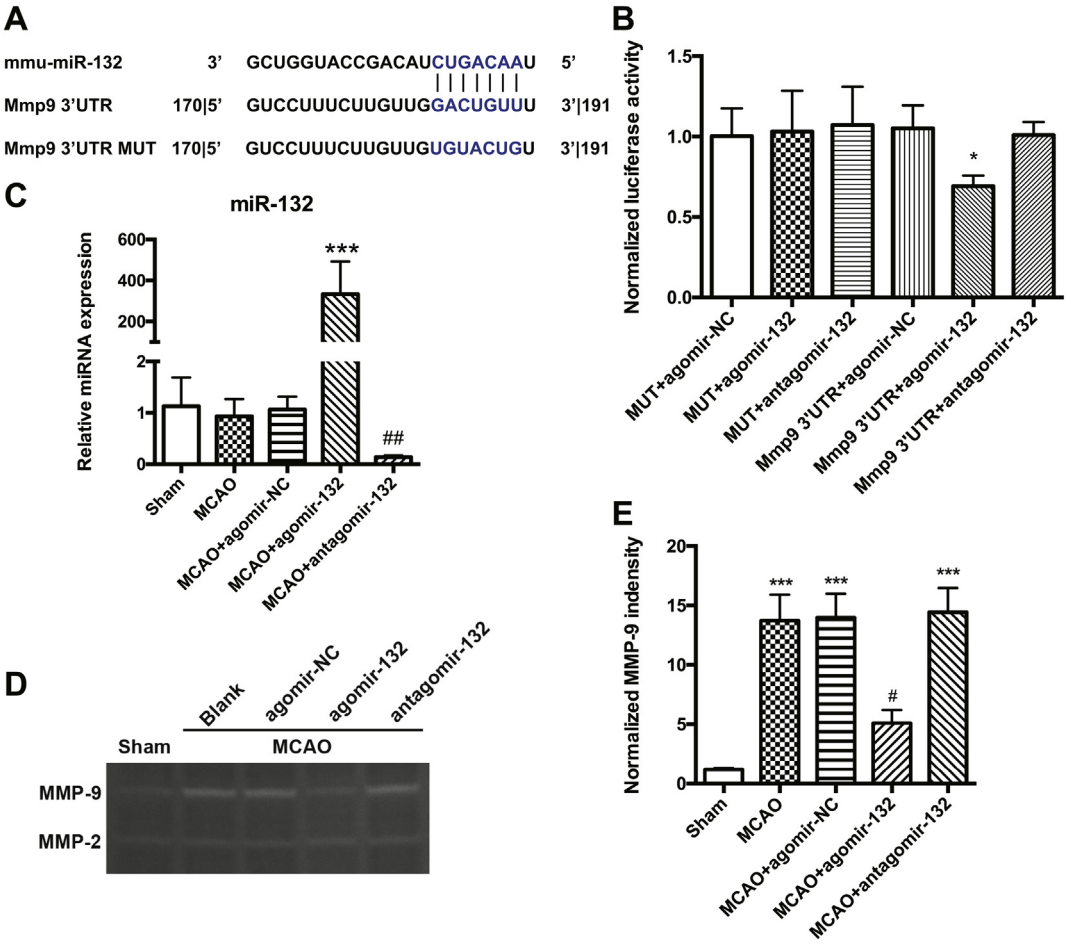

Fig. 5. Mir-132 regulated blood-brain barrier integrity by directly targeting *Mmp9*. (A) Schematic showing potential mir-132 binding site of *Mmp9* 3′UTR. Mutant of Mmp9 3′UTR was introduced by replacing the wildtype binding sequence (GACUGUU) with a mutant sequence (UGUACUG). (B) Suppression of the relative luciferase activity of the Mmp9 3′UTR reporter in CHO cells by mir-132. (C) Level of mir-132 extremely increased after the injection of agomir-132. (D) Gelatinase assay revealed decreased MMP-9 activity in MCAO + agomir-132 group. (E) Quantitative analysis of MMP-9 activity in different groups. $^{*}p < .05$ vs. Sham, $^{***}p < .001$ vs. Sham, $^{\#}p < .05$ vs. MCAO + agomir-NC, $^{\#\#\#}p < .001$ vs. MCAO + agomir-NC, $^{\&\&}p < .001$ in MCAO + antagomir-132 vs MCAO + agomir-NC. Values are presented as Mean ± SD, n = 6 per group.

those protection effects. We were able to demonstrate that the administration of agomir-132 decreased the infarct volume, reduced the permeability of BBB, and improved the neurological functions of mice after MCAO. The benefits of agomir-132 were abolished by administration of antagomir-132. We further demonstrated that agomir-132 directly targeted *Mmp9* and suppressed its expression, consequently reducing degradation of tight junction proteins VE-cadherin and β-catenin and maintaining the integrity of BBB. These observations indicated that miR-132 might serve as an alternative therapeutic strategy to alleviate brain injury in ischemic stroke patients by protecting BBB.

BBB separates the brain tissue from the blood circulation and protects the central nervous system against harmful substances. Endothelial cells and tight junction proteins between them largely regulate the permeability of BBB (Daneman and Prat, 2015; Pang et al., 2017). After ischemic stroke, the integrity of BBB is significantly impaired, which plays an important role in the pathophysiology of stroke (Luh et al., 2018; Sandoval and Witt, 2008). The degradation of tight junction proteins leads to BBB dysfunctions and permits the influx of neutrophils, immune cells and inflammatory factors, leading to inflammation and brain edema (Alluri et al., 2016). MMPs, especially MMP-9 and MMP-2 overexpression have been claimed to be the major perpetrators in BBB disruption (Navarro-Oviedo et al., 2018; Sang et al., 2017). Stabilization of BBB after stroke is protective. It reduces neuronal damage and improves neurological functions (Abdullahi et al., 2018; Chen et al., 2018). Our results showed that the activity of MMP-9 greatly increased 24 h after MCAO. That was accompanied whit degradation of tight junction proteins VE-cadherin and β-Catenin, and consequently with the increase of BBB permeability and development of brain edema. These findings are in accordance with previous studies (Xu et al., 2017). Furthermore, we found that the administration of exogenous miR-132 2 h before MCAO suppressed the expression of MMP-9 leading to protection of the BBB integrity and reduction of brain edema.

miR-132 is abundantly expressed in the central nervous system and plays a critical role in neurodevelopment , synaptic plasticity, and neuronal death (Edbauer et al., 2010). Recently, studies have shown that miR-132 is involved in the pathophysiology of stroke, especially in the regulation of BBB integrity (Che et al., 2018; Zhang et al., 2017). In ischemic stroke patients, the expression of miR-132 in blood was lower than healthy volunteers, and overexpression miR-132 in PC12 cells with oxygen glucose deprivation (OGD) model suppressed the NF-κB pathway and promoted the VEGF pathway (Che et al., 2018). In primary cultures of hippocampal CA1 neurons, ischemia induced epigenetic remodeling at the miR-132 promoter and silencing of miR-132 expression; overexpression of miR-132 by lentivirus protected CA1 neurons from ischemia-induced death in transient global ischemic rats (Hwang et al., 2014). In larval zebrafish, Xu et al. found that MiR-132 knockdown and mutation impaired brain vascular integrity, and neurons can translocate miR-132 to endothelial cells through secreting exosomes to regulate the expression of tight junction protein Cdh5 (Xu

et al., 2017). Accumulating evidences indicates that MMP-9, an endopeptidase that degrades extracellular matrix proteins is one of the direct targets of miR-132 (Jasinska et al., 2016; Ucar et al., 2010). Given that miR-132 exerted their functional effects via the suppression of target gene expression, we examined the effects of agomir-132 and antagomir-132 on the expression of MMP-9 mRNA by luciferase reporter system. Administration of exogenous agomir-132 greatly increased the level of miR-132 in the brain tissue, and suppressed MMP-9 mRNA as well as its protein secretion, which was reverted by administration of antagomir-132. Furthermore, we demonstrate that the overexpression of miR-132 by exogenous agomir-132 reduced the degradation of tight junction proteins VE-cadherin and β-catenin. The impairment of BBB integrity leads to the extravasation of leucocytes and inflammatory mediators into the brain, ultimately results in neuroinflammation and brain edema (Zhou et al., 2018). Administration of exogenous agomir-132 effectively alleviated the destruction of tight junction proteins, attenuated brain edema and improved neurological deficits. Taken together, we provided the evidence that miR-132 regulates the integrity of BBB through suppressing MMP-9 mRNA in MCAO mice. Our study revealed a new signal pathway correlating miR-132 and MMP-9 after MCAO. It proved a new sight of microRNA impact on stroke.

5. Conclusion

The present findings proved that administration of exogenous agomir-132 guarded BBB integrity through suppressing the expression of MMP-9 mRNA and reducing the degradation of VE-cadherin and β-Catenin in ischemic stroke mice. MiR-132/MMP-9 axis might be a novel therapeutic target for BBB protection in various neurological conditions, especially for ischemic stroke in which the permeability of BBB greatly increased. Application of exogenous agomir-132 may be a potential strategy for alleviating BBB damage in neurological and cerebrovascular diseases.

Acknowledgement

This study was supported by grants from the National Natural Science Foundation of China No. 81671130 to Qin Hu and No. 81760234 to Ying Xia, and from Shanghai Municipal Science and Technology Commission Medical Guidance Science and Technology Support Project, NO: 19411968400 to Qiyong Mei.

Competing interests

The authors declare that they have no competing interests.

Appendix A. Supplementary data

Supplementary data to this article can be found online at https://doi.org/10.1016/j.expneurol.2019.03.017.

References

Abdullahi, W., Tripathi, D., Ronaldson, P.T., 2018. Blood-brain barrier dysfunction in ischemic stroke: targeting tight junctions and transporters for vascular protection. Am. J. Phys. Cell Phys. 315, C343–C356.

Alluri, H., Grimsley, M., Anasooya Shaji, C., Varghese, K.P., Zhang, S.L., Peddaboina, C., Robinson, B., Beeram, M.R., Huang, J.H., Tharakan, B., 2016. Attenuation of blood-brain barrier breakdown and hyperpermeability by Calpain inhibition. J. Biol. Chem. 291, 26958–26969.

Bell, J.D., Cho, J.E., Giffard, R.G., 2017. MicroRNA changes in preconditioning-induced neuroprotection. Transl. Stroke Res. 8, 585–596.

Cassidy, J.M., Cramer, S.C., 2017. Spontaneous and therapeutic-induced mechanisms of functional recovery after stroke. Transl. Stroke Res. 8, 33–46.

Che, F., Du, H., Zhang, W., Cheng, Z., Tong, Y., 2018. MicroRNA-132 modifies angiogenesis in patients with ischemic cerebrovascular disease by suppressing the NFkappaB and VEGF pathway. Mol. Med. Rep. 17, 2724–2730.

Chen, H.S., Chen, X., Li, W.T., Shen, J.G., 2018. Targeting RNS/caveolin-1/MMP signaling cascades to protect against cerebral ischemia-reperfusion injuries: potential application for drug discovery. Acta Pharmacol. Sin. 39, 669–682.

Daneman, R., Prat, A., 2015. The blood-brain barrier. Cold Spring Harb. Perspect. Biol. 7, a020412.

Edbauer, D., Neilson, J.R., Foster, K.A., Wang, C.F., Seeburg, D.P., Batterton, M.N., Tada, T., Dolan, B.M., Sharp, P.A., Sheng, M., 2010. Regulation of synaptic structure and function by FMRP-associated microRNAs miR-125b and miR-132. Neuron 65, 373–384.

El Fatimy, R., Li, S., Chen, Z., Mushannen, T., Gongala, S., Wei, Z., Balu, D.T., Rabinovsky, R., Cantlon, A., Elkhal, A., et al., 2018. MicroRNA-132 provides neuroprotection for tauopathies via multiple signaling pathways. Acta Neuropathol. 136, 537–555.

Hu, Q., Manaenko, A., Bian, H., Guo, Z., Huang, J.L., Guo, Z.N., Yang, P., Tang, J., Zhang, J.H., 2017. Hyperbaric oxygen reduces infarction volume and hemorrhagic transformation through ATP/NAD(+)/Sirt1 pathway in hyperglycemic middle cerebral artery occlusion rats. Stroke 48, 1655–1664.

Huang, S., Zhao, J.P., Huang, D.X., Zhuo, L.P., Liao, S.Q., Jiang, Z., 2016. Serum miR-132 is a risk marker of post-stroke cognitive impairment. Neurosci. Lett. 615, 102–106.

Hwang, J.Y., Kaneko, N., Noh, K.M., Pontarelli, F., Zukin, R.S., 2014. The gene silencing transcription factor REST represses miR-132 expression in hippocampal neurons destined to die. J. Mol. Biol. 426, 3454–3466.

Jasinska, M., Milek, J., Cymerman, I.A., Leski, S., Kaczmarek, L., Dziembowska, M., 2016. miR-132 regulates dendritic spine structure by direct targeting of matrix metalloproteinase 9 mRNA. Mol. Neurobiol. 53, 4701–4712.

Koh, S.H., Park, H.H., 2017. Neurogenesis in stroke recovery. Transl. Stroke Res. 8, 3–13.

Lapchak, P.A., Zhang, J.H., 2017. The high cost of stroke and stroke cytoprotection research. Transl. Stroke Res. 8, 307–317.

Lapchak, P.A., Lara, J.M., Boitano, P.D., 2017. Cytoprotective drug-tissue plasminogen activator protease interaction assays: screening of two novel cytoprotective chromones. Transl. Stroke Res. 8, 494–506.

Li, G., Morris-Blanco, K.C., Lopez, M.S., Yang, T., Zhao, H., Vemuganti, R., Luo, Y., 2018. Impact of microRNAs on ischemic stroke: from pre- to post-disease. Prog. Neurobiol. 163-164, 59–78.

Lim, T.C., Spector, M., 2017. Biomaterials for enhancing CNS repair. Transl. Stroke Res. 8, 57–64.

Luh, C., Feiler, S., Frauenknecht, K., Meyer, S., Lubomirov, L.T., Neulen, A., Thal, S.C., 2018. The contractile apparatus is essential for the integrity of the blood-brain barrier after experimental subarachnoid hemorrhage. Transl. Stroke Res. 1–12. https://doi.org/10.1007/s12975-018-0677-0.

Miller, B.H., Zeier, Z., Xi, L., Lanz, T.A., Deng, S., Strathmann, J., Willoughby, D., Kenny, P.J., Elsworth, J.D., Lawrence, M.S., et al., 2012. MicroRNA-132 dysregulation in schizophrenia has implications for both neurodevelopment and adult brain function. Proc. Natl. Acad. Sci. U. S. A. 109, 3125–3130.

Navarro-Oviedo, M., Roncal, C., Salicio, A., Belzunce, M., Rabal, O., Toledo, E., Zandio, B., Rodriguez, J.A., Paramo, J.A., Munoz, R., et al., 2018. MMP10 promotes efficient thrombolysis after ischemic stroke in mice with induced diabetes. Transl. Stroke Res. 1–12. https://doi.org/10.1007/s12975-018-0652-9.

Pang, J., Chen, Y., Kuai, L., Yang, P., Peng, J., Wu, Y., Chen, Y., Vitek, M.P., Chen, L., Sun, X., et al., 2017. Inhibition of blood-brain barrier disruption by an apolipoprotein E-mimetic peptide ameliorates early brain injury in experimental subarachnoid hemorrhage. Transl. Stroke Res. 8, 257–272.

Rink, C., Khanna, S., 2011. MicroRNA in ischemic stroke etiology and pathology. Physiol. Genomics 43, 521–528.

Sandoval, K.E., Witt, K.A., 2008. Blood-brain barrier tight junction permeability and ischemic stroke. Neurobiol. Dis. 32, 200–219.

Sang, H.F., Qiu, Z.M., Cai, J., Lan, W.Y., Yu, L.J., Zhang, H., Li, M., Xie, Y., Guo, R.B., Ye, R.D., et al., 2017. Early increased bradykinin 1 receptor contributes to hemorrhagic transformation after ischemic stroke in type 1 diabetic rats. Transl. Stroke Res. 8, 597–611.

Ucar, A., Vafaizadeh, V., Jarry, H., Fiedler, J., Klemmt, P.A., Thum, T., Groner, B., Chowdhury, K., 2010. miR-212 and miR-132 are required for epithelial stromal interactions necessary for mouse mammary gland development. Nat. Genet. 42, 1101–1108.

Xu, B., Zhang, Y., Du, X.F., Li, J., Zi, H.X., Bu, J.W., Yan, Y., Han, H., Du, J.L., 2017. Neurons secrete miR-132-containing exosomes to regulate brain vascular integrity. Cell Res. 27, 882–897.

Zhang, Y., Han, B., He, Y., Li, D., Ma, X., Liu, Q., Hao, J., 2017. MicroRNA-132 attenuates neurobehavioral and neuropathological changes associated with intracerebral hemorrhage in mice. Neurochem. Int. 107, 182–190.

Zhou, Z.H., Lu, J.F., Liu, W.W., Manaenko, A., Hou, X.H., Mei, Q.Y., Huang, J.L., Tang, J.P., Zhang, J.H., Yao, H.H., et al., 2018. Advances in stroke pharmacology. Pharmacol. Therapeut. 191, 23–42.